

Pluto's climate modeled with new observational constraints



C.J. Hansen^{a,*}, D.A. Paige^b, L.A. Young^c

^a Planetary Science Institute, 389 N. Industrial Rd., Suite 5, St. George, UT 84770, United States

^b University of California, Los Angeles, CA 90095, United States

^c Southwest Research Institute, Boulder, CO 80302, United States

ARTICLE INFO

Article history:

Received 20 December 2013

Revised 2 March 2014

Accepted 5 March 2014

Available online 27 March 2014

Keywords:

Pluto, atmosphere

Pluto, surface

Atmospheres, evolution

Ices

ABSTRACT

Pluto has a nitrogen atmosphere in vapor pressure equilibrium with surface ice. N₂ is mobile and is transported seasonally even at Pluto's cold temperatures in the outer Solar System. A thermal model developed by Hansen and Paige in 1996 to model Pluto's climate has been re-deployed in response to new data and in anticipation of the New Horizons flyby of Pluto in 2015. A number of stellar occultations have been observed in the last 11 years as Pluto has crossed the galactic plane. New Hubble Space Telescope images show a variegated surface. These recent observations allow us to model Pluto's climate with much tighter constraints. Our findings suggest that Pluto's atmosphere will not collapse prior to the arrival of New Horizons although pressure will be dropping as N₂ condenses on the south polar cap. This finding is in contrast to the Olkin et al. (Olkin et al. [2013], arXiv1309.08410) prediction that permanent volatiles in the northern hemisphere maintain Pluto's atmospheric pressure throughout its orbit. The range of surface pressures predicted for 2015 for nine cases with very good matches to observables is 0.3–3.2 Pa. The best match predicts that New Horizons will detect an atmospheric pressure of 2.4 Pa.

© 2014 Elsevier Inc. All rights reserved.

1. Introduction

In the cold outer Solar System Pluto and Triton have nitrogen atmospheres in vapor pressure equilibrium with surface ices (Pluto: Stern and Trafton, 1984; Elliot et al., 1989; Hubbard et al., 1990; Owen et al., 1992, 1993; Hansen and Paige, 1996; Triton: Trafton, 1984; Spencer, 1990; Hansen and Paige, 1992; Spencer and Moore, 1992). Volatile nitrogen sublimates from the pole experiencing spring and condenses on the pole in autumn. This seasonal transport affects the pressure of the atmosphere, the location of polar cap boundaries (thus the albedo as seen from the Earth), and the surface temperatures. In their outer Solar System outposts, these two bodies are often compared to each other – one a Kuiper Belt Object (KBO) in an eccentric orbit in an orbital resonance with Neptune, and the other a captured KBO now in orbit around Neptune.

New Earth-based observations inform and constrain what we know about Pluto's climate and motivate updates to old climate models in anticipation of the New Horizons flyby of Pluto in 2015. One volatile transport model to which observations have been frequently compared was originally developed by Hansen and Paige for Triton (Hansen and Paige, 1992), and modified for Pluto in 1996 (Hansen and Paige, 1996, referred to hereafter as

HP96). This finite-element parameterized thermal model balances and conserves energy across the body while tracking locations and quantities of N₂ sublimation and condensation in and out of the atmosphere. The model successfully predicted the increase in pressure of Pluto's atmosphere even as Pluto moved away from perihelion (Sicardy et al., 2003; Elliot et al., 2003). Note that throughout this paper the terms “frost” and “ice” are used interchangeably, and in all cases refer to condensed N₂.

Stellar occultations are key to understanding the composition and structure of Pluto's atmosphere (Elliot and Young, 1991; Sicardy et al., 2003; Young et al., 2010). At the time that HP96 was developed there was just one measurement of atmospheric pressure from a stellar occultation in 1988 (Elliot et al., 1989; Hubbard et al., 1990) to compare with model output. In the last 11 years however as Pluto has crossed the galactic plane numerous occultations have been observed.

Mutual eclipses and occultations between Pluto and Charon in the late 1980s allowed derivation of coarse albedo maps of Pluto's disk (Buie et al., 1992; Young and Binzel, 1993) – these were compared to predicted polar cap boundaries by HP96. Now disk-resolved images from Hubble Space Telescope (HST) give a more complete picture of Pluto's surface.

With over 20 years of new observations and the imminent arrival of New Horizons at Pluto (Young, 2013) it is time to take a new look at Pluto's climate.

* Corresponding author.

E-mail address: cjhansen@psi.edu (C.J. Hansen).

2. New observational data

When the HP96 model was developed Pluto observations were sparse: a single occultation in 1988, and the albedo map derived from the Pluto–Charon mutual events provided the primary constraints. In the years since the original results were published many more observations of Pluto have been acquired. Four important observational categories, described in this section, serve to constrain Pluto's surface and ice properties such that predictions can be made for the state of Pluto's climate at the time the New Horizons spacecraft passes by.

2.1. Resolved albedo maps

N_2 is a very mobile species even at Pluto's cold temperatures. It will sublime and condense quickly as the subsolar latitude changes. From telescopes on and in orbit around the Earth volatile redistribution will manifest itself as changes in both disk-integrated brightness and resolved albedo maps. The viewing geometry from the Earth must be taken into account – when Pluto was first discovered Earth-based observers were looking at the south pole. (We follow the Pluto community and current IAU convention of defining north as the direction of the angular momentum vector of the planet.) A large polar cap (or no polar cap) would give a flat light curve and a very slow change in overall brightness as the Sun (and Earth) moved toward the equator – comparison of overall brightness accounting for the change in distance is just a 5% darkening from 1933 to 1953 (Schaefer et al., 2008), over a period of time that the subsolar latitude was fairly constant. After 1953, as the south pole rotated out of view the amplitude of the light curve over a Pluto rotation increased (e.g. Binzel and Mulholland, 1983; Marcialis, 1988), consistent with more longitudinal heterogeneity on the surface becoming visible from Earth. At the time of the mutual events ground-based observers were looking roughly at the equator and could discern a bright south pole, but results for the north polar region were mixed, with one group deriving a bright north polar region (Young and Binzel, 1993) and the other not (Buie et al., 1992).

With the resolution of the Hubble Space Telescope bright north and south poles could be discerned in 1994 (Stern et al., 1997; Buie et al., 2010b), with the north polar region larger in extent. A bright north polar region was visible in 2003, with the south pole rotated out of view as seen from the Earth (Buie et al., 2010b). As more of the north pole comes into view the light-curve amplitude is beginning to decrease again (Buie et al., 2010a).

Most importantly, HST maps show a longitudinally variegated surface (Stern et al., 1997; Buie et al., 2010b; Lellouch et al., 2011a,b). The longitudinal heterogeneity in albedo provides a strong constraint on surface properties as described in Sections 3 and 5.

2.2. Stellar occultations

A stellar occultation in 2002 broke the long hiatus after 1988. This occultation revealed that Pluto's atmospheric pressure had approximately doubled (Elliot et al., 2003; Sicardy et al., 2003; Paschoff et al., 2005). With Pluto crossing the galactic plane, occultations in 2006, 2007, 2008, 2009, and 2010 were observed (summarized in Young, 2013). New data from occultations observed in 2011, 2012 and 2013 (Person et al., 2013; Bosh et al., 2013; Olkin et al., 2013, resp.) are now being analyzed.

Interpretation of occultation data is challenging however, due to the structure of the lowest part of the occultation light curve – it can be attributed to either a steep thermal gradient or a haze layer in the atmosphere (Elliot and Young, 1992; Eshleman,

1989; Hubbard et al., 1990; Stansberry et al., 1994; Young et al., 2008). This leads to uncertainty in Pluto's radius and the value of the atmospheric pressure at the surface. Although the pressures are routinely reported for an altitude of 1275 km, surface pressures extrapolated below that altitude can be bracketed as in Young (2013). Pressures at the reference altitude can also be compared to each other, e.g. the atmospheric pressure detected in 2006 was 1.5–3 times the pressure in 1988 (Elliot et al., 2007).

Occultation data through 2008 are clearly consistent with secularly increasing atmospheric pressure, with pressure in 2009–2010 increasing slightly or leveling off (Sicardy personal communication, 2013; Young, 2013). New results from the most recent stellar occultations in 2012 and 2013 were reported at the 2013 Pluto Science Conference (“The Pluto System on the Eve of Exploration by New Horizons: Perspectives and Predictions”). The observations show that Pluto's atmospheric pressure has increased compared to 2011 (Olkin et al., 2013; Sicardy, personal communication, 2013), or stayed constant (Person et al., this issue, 2013 – note that this group reports pressure at half light rather than 1275 km).

All simulations were passed through the same wide sieve used by Young (2013), to identify those results roughly consistent with stellar occultations in 1988 and 2006. The rationale for the sieve is expanded here, relative to Young (2013). The wide sieve used 1988 and 2006, rather than 1988 and 2002, because of the relatively large error bars on the 2002 retrieved pressures. The range of acceptable pressures for 2006 was taken to be 7–78 μbar . The lower end of the range is dictated by the fact that occultations in 2006 probed down to at least 6 μbar (Young et al., 2008). The upper end of the range is guided by Lellouch et al. (2009), who combined high-resolution IR spectra of Pluto's gaseous CH_4 with stellar occultations to derive a maximum pressure in 2008 of 24 μbar . The larger upper end of the 2006 sieve range accounts for the difference in time between 2006 and 2008, and the model dependence of the Lellouch et al. (2009) result.

Young et al. (2008) report that the pressure in 2006 at a reference radius of 1275 km from Pluto's center was a factor of 2.4 ± 0.3 times larger than in 1988. Taking into account the difficulty in relating pressure at 1275 km to Pluto's surface, spanning a gap of some 75–100 km, the sieve requires a ratio of the 2006 and 1988 surface pressures in the range of 1.5–3.1. The limits on the ratio of pressures would imply a range for 1988 of 2.2–52 μbar . However, the stellar occultation of 1988 provides an additional constraint, as it probed to 3.0 μbar . The final 1988 pressure range for the sieve is 3.0–52 μbar .

2.3. Surface properties and temperature

Thermal modeling allowed Pluto's surface (diurnal skin depth) thermal inertia to be derived from Spitzer data obtained in 2004. The derived inertia, 20–30 $\text{J/m}^2 \text{s}^{1/2} \text{K}$, is lower than values expected for compact ices, possibly due to high surface porosity (Lellouch et al., 2011a). Lellouch et al. derive a temperature at the subsolar point of $\sim 63 \text{K}$ in 2004 for their best-fit values for surface bond albedo and emissivity. Far infrared data acquired from the Infrared Astronomical Satellite (Sykes et al., 1987; Sykes, 1993) constrains the surface temperature to be in the range of 55–73 K in 1983.

2.4. Other ices

In addition to the very volatile N_2 ice, the ices CO , and CH_4 have also been detected spectroscopically on Pluto's surface (Cruikshank et al., 1976; Owen et al., 1993). The spectra is generally interpreted as indicating three broad terrain types (e.g., Grundy and Buie, 2001; Lellouch et al., 2011a): a large-grained terrain with dilute CO and CH_4 , indicated by the N_2 feature at 2.15 μm , CO absorption,

and shifted CH₄ lines; a pure or nearly pure CH₄ terrain that may also contain dilute CO and N₂, indicated by essentially unshifted CH₄ lines; and a third spectrally bland terrain. The third terrain type was originally modeled as bright and spectrally neutral fine-grained pure N₂ (Douté et al., 1999) to match near-IR spectra, but combined near-IR and mid-IR spectra from 2001 to 2002 support the interpretation of the third terrain being tholin rather than fine-grained N₂ ice (Olkin et al., 2007). While it is difficult to unambiguously relate the equivalent widths of bands to spatial coverage, Grundy et al. (2014) find a secular decrease in the N₂ and CO band width between 2001 and 2012, with a change in the rate suggestive of a receding polar cap.

The HP96 model does not include CH₄ explicitly however we can look for albedo trends indicative of a receding north polar cap between 2001 and 2012. We can also compare our model surface temperature predictions to temperatures of 41 K for the CH₄ highly diluted in N₂ and 60 K for the pure methane temperature derived by Olkin et al. (2007) as the best fit to their 2003 data.

3. Pluto's seasons

Pluto is in an eccentric orbit around the Sun (eccentricity = 0.2482). It has an obliquity of 122.46°, or effectively ~58°. Both of these geometric parameters affect insolation and thus have consequences for the volatile distribution on the surface and partitioning of N₂ between surface ices and the atmosphere.

Pluto crossed perihelion in 1989. One might expect that as Pluto moved away from perihelion its atmospheric pressure would drop steadily. The HP96 model however predicted a boost in atmospheric pressure, with the expected drop delayed to ~2025. The reason for this is illustrated in Fig. 1 – Pluto's obliquity matters. The subsolar point crossed the equator in 1988, within a year of perihelion in 1989. Since then the frost-covered north polar regions have been increasingly illuminated and solar insolation is causing the frost in the northern hemisphere to sublime. Sublimation in the north is occurring more rapidly than condensation of

frost in the south polar region, increasing the amount of N₂ in the atmosphere. Comparisons to stellar occultation data are generally consistent with this HP96 prediction (Sicardy et al., 2003; Elliot et al., 2003).

Another interesting consequence of Pluto's obliquity is the location of any permanent cold traps. For bodies with low obliquity permanent cold traps will be at the poles. Planets with obliquities greater than ~54° however have annual insolation greater at the poles than at the equator (Ward, 1974). Pluto's obliquity is >54°, which means that a permanent cold trap will be in a zonal latitudinally-confined band of ice, not polar caps. If conditions are such that N₂ ice is cold-trapped in these bands (described in Section 5) the bands persist throughout the Pluto year. Surface albedo does not have any influence once frost has accumulated in the cold trap. In the absence of topography the permanent cold trap will be frost-covered at all longitudes. A prediction of our model with some parameter sets is that N₂ ice at the north pole will disappear before ice at lower latitudes. This development of a "polar bald spot" is also due to Pluto's high obliquity, but in contrast would lead to a temporary zonal band, that would disappear once the polar cap completely sublimated.

4. The climate model

The HP96 model was originally based on the Leighton and Murray (1966) climate model for Mars' CO₂ atmosphere, in vapor pressure equilibrium with surface ices. On Pluto and Triton the atmospheric volatile in vapor pressure equilibrium with surface ice is N₂, which is in either an alpha or beta solid phase, depending on the temperature. Hansen and Paige (1992, 1996) developed a finite-element parameterized thermal model (HP96) that balances and conserves energy across Pluto while tracking locations and quantities of N₂ sublimation and condensation in and out of the atmosphere, maintaining mass conservation and consistent with the requirement of vapor pressure equilibrium. As shown in Fig. 2 the energy balance equation consists of 5 components:

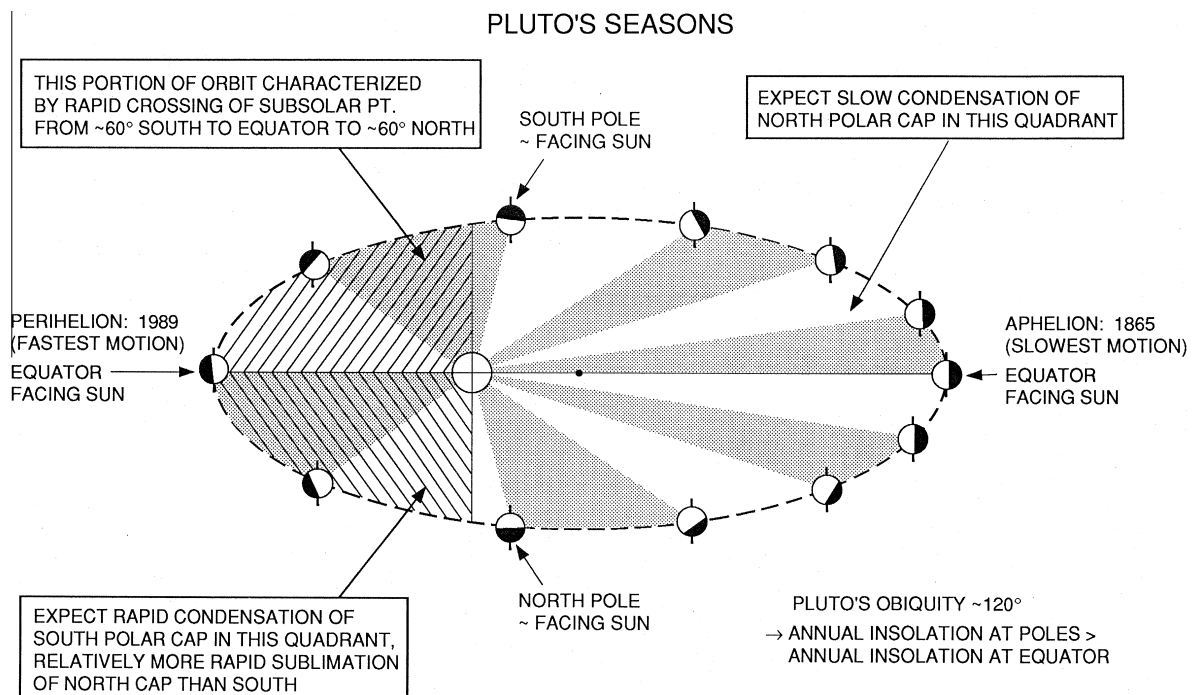


Fig. 1. The eccentricity of Pluto's orbit and Pluto's obliquity have a profound effect on atmospheric pressure and the distribution of volatiles on the surface. (Figure is reproduced from Hansen and Paige, 1996.)

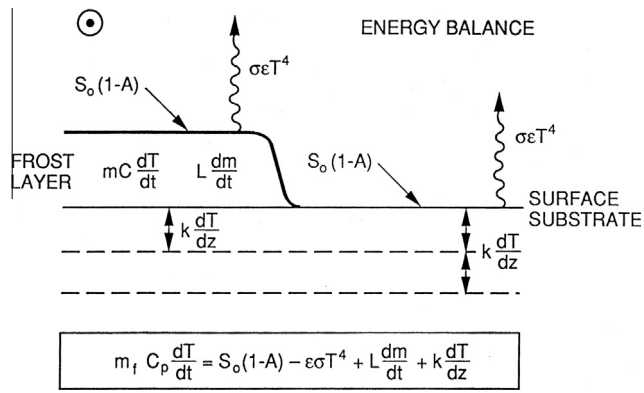


Fig. 2. Basic tenets of the energy balance equation (Hansen and Paige, 1996) are illustrated, as described in the text. N_2 sublimation and condensation in and out of the atmosphere is tracked and mass is conserved. (Figure is reproduced from Hansen and Paige, 1992.)

- solar energy absorbed by the frost and surface: $S_0(1 - A)$, where S_0 is incident solar energy and A is the Bond albedo;
- energy emitted from the surface and frost: $\epsilon \sigma T^4$, where ϵ is the emissivity of the frost or surface, σ is the Stefan–Boltzmann constant, and T is the temperature;
- energy conducted to and from the subsurface: $k dT/dz$, where k is the conductivity of the substrate and dT/dz is the thermal gradient;
- latent heat of sublimation and condensation: $L dm/dt$, where L is the latent heat and dm/dt is the amount of N_2 condensed or sublimed in the time step;
- the change in temperature of the frost layer $m C dT/dt$, where m is the mass of the frost in kg/m^2 , C is the specific heat.

Below the surface heat transport is treated as a diffusive process. Each time the energy balance equation is solved there are two unknowns: dm/dt and dT/dt . To solve the equation we apply the constraint of vapor pressure equilibrium. At any given latitude and time there is a unique combination of values for dm/dt and dT/dt such that the change in frost temperature, the amount of frost sublimed or condensed, and the frostpoint temperature that corresponds to the newly calculated atmospheric pressure are consistent with local conservation of energy, global conservation of mass, and vapor pressure equilibrium. The model is designed to seamlessly transition between cases where the atmospheric pressure is high enough to buffer surface frost temperatures, and cases where atmospheric pressures become negligible and surface frost temperatures are determined by insolation and thermal conduction.

S_0 is determined by the latitude, orbit of the body, period of rotation, and obliquity, which are all inputs to the model. Light reflected or emitted from Charon is not included. Most model runs are for 10–20 Pluto years. The latent heat, L , is determined by whether the N_2 ice is in the alpha or beta phase. Input parameters that are varied are frost albedo and emissivity, surface albedo and emissivity, thermal inertia, subsurface conductivity, and N_2 inventory.

The model outputs include atmospheric pressure, frost distribution on the surface (polar cap boundaries), physical temperature of the surface, and frostpoint temperature, as a function of time. Fig. 3 shows an example plot. These predictions can be compared to observables as seen from the Earth: pressure, albedo maps, disk-integrated albedo, and thermal emission at a given wavelength. The aspect angle of the body as seen from the Earth is accounted for in the calculation of disk-integrated albedo and thermal emission.

5. General trends

With limited data to constrain the results, the HP96 effort tested a vast multi-dimensional parameter space. Frost and surface albedos were varied from 0.2 to 1.0. Frost emissivity was varied from 0.2 to 1.0. Surface thermal inertia values were varied from 1 (“low”) to 50 (“high”) $\times 10^{-3}$ cal/($cm^2 s^{1/2} K$). The nitrogen inventory was set at 50, 100 or 200 kg/m^2 .

Interesting general trends emerged. Pluto’s annual average insolation is higher at its poles than at its equator because of its obliquity, so latitudinally constrained (“zonal”) bands of ice are produced whenever the frost mobility is reduced. This happens when the frost is cold, due to either high albedo or high emissivity. Likewise, zonal bands are more likely when the thermal inertia is high. Higher thermal inertia surfaces require longer to cool off or to warm up, and thus remain closer to their annual average temperatures. Zonal bands are also the permanent location for any N_2 inventory higher than the amount that can be redistributed seasonally. In this case runs produced zonal bands with seasonal polar caps. Even when the longitude of perihelion is rotated, as is the case with the 300 MY precession of Pluto’s orbit, the permanent cold trap is a zonal band.

Two peaks in atmospheric pressure per year were always predicted for runs without zonal bands, associated with the sublimation of the polar caps. The peak produced by the sublimation of the northern polar cap is always larger (in this epoch with the current longitude of perihelion). The presence of a permanent zonal band flattens out the peaks. A low thermal inertia surface enhances the peaks as temperature changes quickly in response to insolation changes.

Variations of surface emissivity were tested. Values less than 1.0 had the general effect of raising the substrate temperature. Surface emissivity = 1 is consistent with arguments made by Lellouch et al. (2011a), if the surface is water ice.

6. New model runs and comparisons

The HP96 model was not changed at all for this new set of runs. Advances in computer speed and computer memory however allowed us to increase the duration of the runs from 10 Pluto years (~ 4400 Earth years, culminating at 2100 AD) to 20 Pluto years. This change enhanced the stability of the results.

HST images show that Pluto has a longitudinally variegated albedo. The lack of bright zonal bands in HST albedo maps immediately eliminates large swaths of parameter space explored by HP96. All cases classified as “high” thermal inertia surfaces by HP96 can be discarded. Even the thermal inertia range considered “moderate” by HP96 failed in many instances. All cases that produce cold frost can be discarded. Fig. 4 shows an example of one such case. The nitrogen inventory can be constrained to <75 kg/m^2 . If the N_2 inventory is too high the excess frost winds up sequestered in zonal bands; if the N_2 inventory is too low the atmospheric pressure is too low.

Constraints from the stellar occultation data collected from 2002 to 2010 were applied next. Parameter space was narrowed considerably by Young (2013), which guided the efforts reported here. Starting with the promising set of conditions identified in Young (2013), over 80 runs have been compared to the occultation pressure values to find conditions that reproduce the observations. The latest stellar occultation results reported at the 2013 Pluto Conference require that the atmospheric pressure increases or stays flat in 2012–2013, but definitely does not decrease (Olkin et al., 2013; B. Sicardy, personal communication, 2013; Person et al., this issue, 2013).

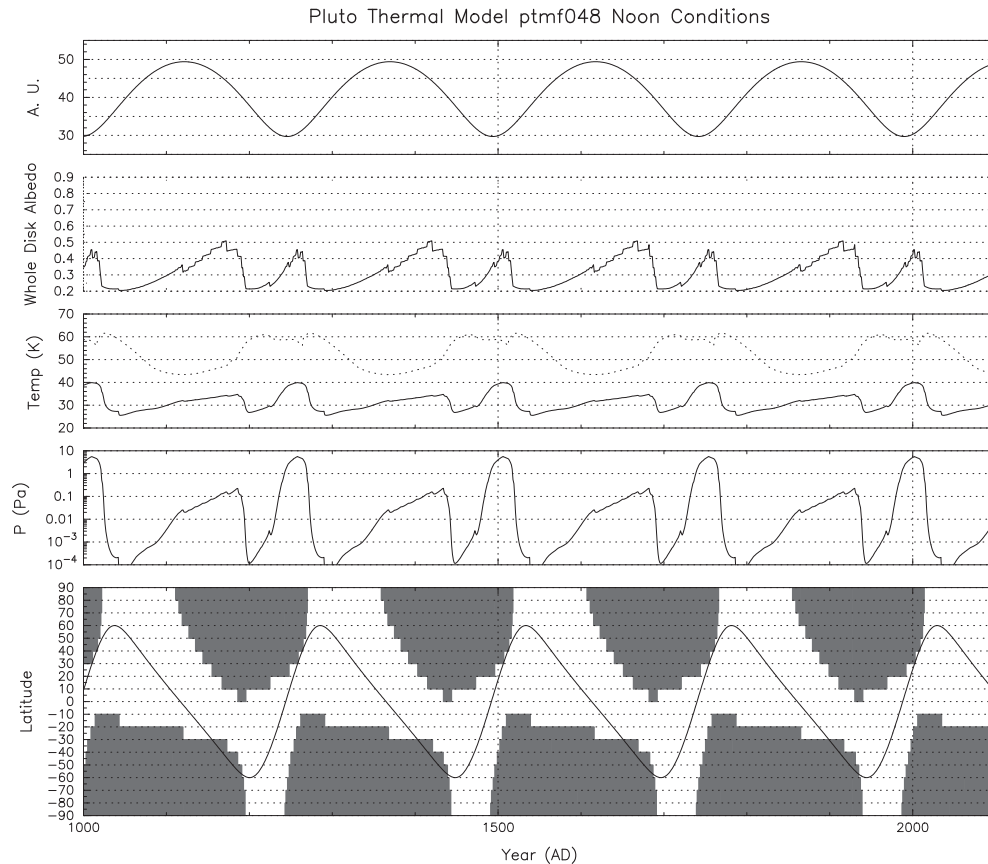


Fig. 3. Results from model run 48 (modeled parameters given in Table 3) are illustrated from 1000 to 2100 AD, or ~ 4.5 Pluto years (the total time span modeled was 20 Pluto years). The top panel shows Pluto's distance from the Sun as a function of time. Pluto's last perihelion passage was in 1989. The second panel gives the disk-integrated albedo as it would be seen from the Earth, taking into account how much bare surface vs. how much frost-covered surface is visible given the sub-Earth latitude as a function of time and the predicted frost distribution. The third panel shows two temperatures: the frost point (solid line) and the temperature of the warmest latitude zone on the surface (dashed line). The temperatures swing with the distance of Pluto from the Sun but are additionally modulated by the season, due to Pluto's obliquity, which results in two temperature peaks per Pluto year. The fourth panel illustrates atmospheric pressure, which varies in this case by over 5 orders of magnitude. The line in the bottom panel shows the subsolar latitude as a function of time. The Sun goes quickly from south to north as Pluto passes through perihelion. It goes slowly from north to south in the aphelion portion of Pluto's orbit, allowing the south polar cap to be in place longer than the north. The stippled areas are covered with frost.

Reproduction of the observations of polar caps was the next criteria applied. The observation of a bright south polar region in 1988 is far more discriminative after the atmospheric pressure constraints are met than the observations of caps in 1994 and a north polar cap in 2003. There are no cases at all in which a bright south polar cap persists through southern summer from 1933 to 1988. The only way to produce a bright south polar cap in 1988 is to have the new seasonal cap start condensing by then as the latitude of the subsolar point moves to the northern hemisphere. In 1994 the north polar cap should be larger in latitudinal extent than the south polar cap, to be consistent with the HST images acquired in 1994 (Stern et al., 1997). We looked for any indication of rapid change between 2000 and 2003, which could explain the color changes noted by Buie et al. (2010a), and for a receding north polar cap between 2001 and 2012.

The next test was to match the temperatures derived from IRTF spectra acquired in 2003 (Olkin, 2007) and the Spitzer data from 2004 (Lellouch et al., 2011a). The 41 K frost temperature should match fairly closely, while the surface temperature should be in the 60–65 K range. Since the temperatures are calculated from models derived to fit spectra and thermal emission, not direct observations, we consider this particular constraint lower in importance than the albedo patterns and stellar occultation observations. The constraints that the surface temperature be in the range 55–73 K in 1983 and that the frost temperature be 40 ± 2 K in 1993 (Tryka et al., 1994) should also be met.

Although our model predicts disk-integrated albedo visible to the ground-based observer, incorporating the sub-Earth latitude and accounting for the changing distance of Pluto from the Sun and Earth, there are several factors that make this a difficult constraint to apply. The model uses bond albedo – to correct that to reflectivity reported by observers one must apply an unknown phase function. Longitude differences are not modeled so comparison to light curves must consistently use maximum, minimum or average, and not some combination. Charon's signal must be separated out. Because of these factors we just compare results to general trends.

Table 2 lists the observational data against which the model results were tested. Parameter sets that did not give these results were rejected.

7. Model results

The increase in atmospheric pressure as the north polar cap sublimates, predicted by HP96, can be sharp and peaked (e.g. Fig. 3) or broad and flat. All cases remaining after zonal-band-producing combinations have been eliminated predict that once the north polar cap reaches a certain point it sublimates quickly. Once the north polar cap is gone the atmospheric pressure drops precipitously.

We now find a narrow range of frost albedo/emissivity values that produce atmospheric pressures in the range of the occultations.

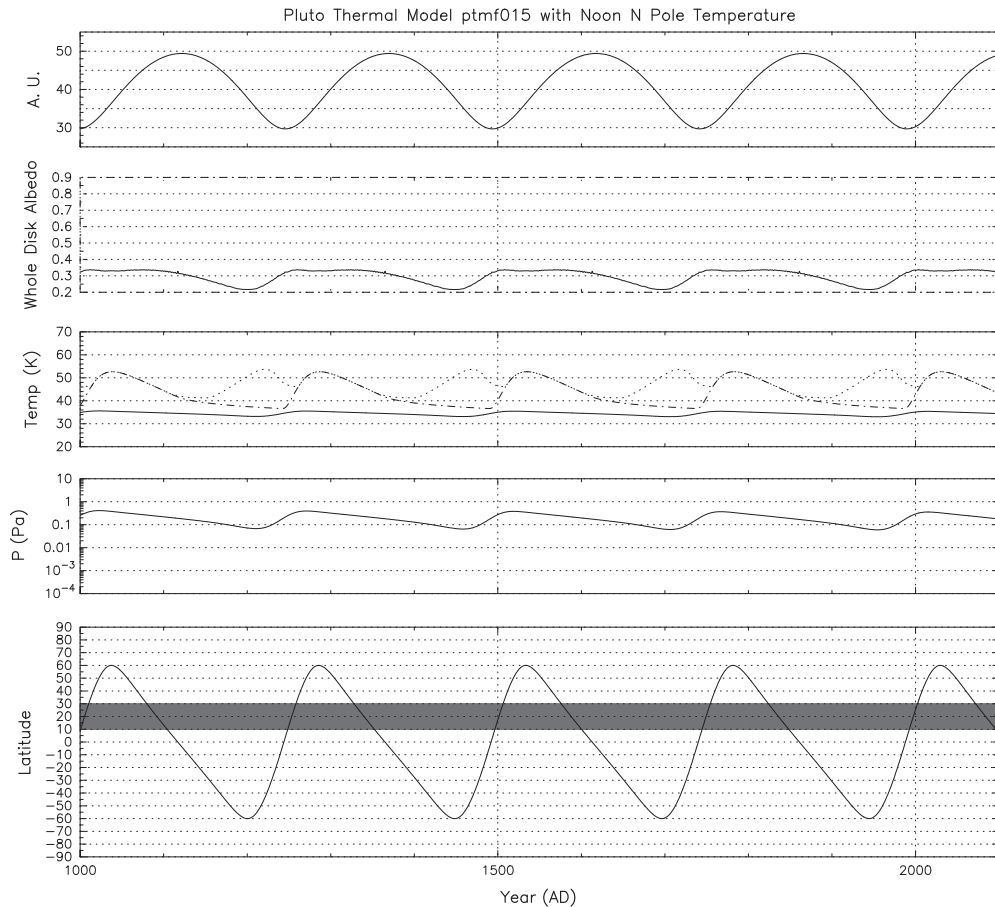


Fig. 4. Run #15 with a thermal inertia of $1000.0 \text{ J/m}^2 \text{ s}^{1/2} \text{ K}$, surface albedo of 0.2, frost albedo of 0.8, frost emissivity of 0.8, and N_2 inventory of 50 kg/m^2 has all its N_2 ice sequestered in a zonal band. Atmospheric pressure modulation exists but it is subdued, and only one peak per Pluto year is observed in northern summer. In this case the N_2 goes in and out of the atmosphere seasonally but the surface stays too warm for it to condense anywhere but in the zonal band. The temperatures plotted in the third panel are the frost point (solid line) and the temperature at the north pole (dot-dash line). Even in the lengthy north polar night the pole never cools quite to the frost point, so seasonal caps are not able to condense. This case is not consistent with the variegated surface observed in HST images.

Table 1

Stellar occultation results used to compare to model predictions. Minimum and maximum surface pressures reflect the ambiguity in how the lowest segment of the occultation data should be interpreted, based on work done in Young (2013), and converted to Pa.

Year of occultation	Minimum surface pressure (Pa)	Maximum surface pressure (Pa)
1988	0.3	5.2
2002	1.3	5.5
2006	0.7	7.8
2007	1.4	6.3
2008	3.0	6.5
2009	1.9	12.7
2010	1.3	5.5

High albedo coupled with high emissivity produces cold frost and atmospheric pressures that are too low. Lower albedo (e.g. 0.6) combined with low emissivity yields warm frost and temperatures, thus pressures that are too high.

Frost emissivity and albedo are coupled in that between the two they control frost temperature, and can compensate for each other: for example a high albedo that would result in a cold frost can be countered by a low emissivity that prevents loss of energy. The combination of frost albedo/emissivity that gives frost temperatures that produce the right pressure to match the occultations from 1988 to 2010 is just (albedo = 0.8/emissivity = 0.55) or (0.7/0.7–0.8), for thermal inertias in the range of $18\text{--}32 \text{ J/m}^2 \text{ s}^{1/2} \text{ K}$.

When the thermal inertia is as low as 10 the frost albedo/emissivity range is further narrowed to (0.8/0.55) or (0.7/0.7). When the thermal inertia is $41 \text{ J/m}^2 \text{ s}^{1/2} \text{ K}$, albedo/emissivity combinations are limited to (0.8/0.6) or (0.7/0.8). We tested increasing thermal inertia to see when the limit of albedo/emissivity combinations is reached that still produces polar caps at the right time, and found that at $64 \text{ J/m}^2 \text{ s}^{1/2} \text{ K}$ we no longer have a south polar cap forming by 1988.

7.1. Good fits to observables

It is very difficult to find parameter combinations that predict a south polar cap in 1988 and atmospheric pressure that is not starting to drop in 2013. High thermal inertia will keep the atmospheric pressure high, but a south polar cap will not start to form by 1988. Lower thermal inertias allow early formation of the south polar cap, but the peak in atmospheric pressure is early in 2002–2008 and pressure is predicted to be starting to decrease by 2013.

Nine cases, listed in Table 3, yielded very good matches to observables. All passed the first three criteria listed in Table 2. None have zonal bands. They all exhibit polar caps in the right places at the right times. All met the criteria of atmospheric pressure given in Table 1. One of these runs, #48, is shown in Fig. 3. Two had a thermal inertia of $41.8 \text{ J/m}^2 \text{ s}^{1/2} \text{ K}$, which would be $1 \times 10^{-3} \text{ cal}/(\text{cm}^2 \text{ s}^{1/2} \text{ K})$ in the units used in HP96. Run #22 was very similar to run 34 of HP96 (Fig. 10 in HP96). All runs have

Table 2

These are the criteria that model results must reproduce, in order for the modeled set of parameters to be a good candidate match to Pluto's actual physical properties.

Observational criteria	Importance
I. No bright zonal bands detected by HST	Model must not predict bands
II. Atmospheric pressure in range defined in Table 1	Model must predict
III. Polar caps at correct places in 1988, 1994 and 2003; north pole receding 2001–2012	Model must predict
IV. Atmospheric pressure in 2006 = $1.5\text{--}3 \times 1988$	Should be close
V. Frost and surface temperatures in 1983, 1993, 2003, and 2004	Closer is better
VI. Steady or increasing atmospheric pressure from 2010 to 2013	Should approximate

the surface emissivity set to 1.0, and have an N_2 inventory of 50 kg/m².

Run 68 was the only run to meet the fourth criteria, IV, that the atmospheric pressure in 2006 should be 1.5–3 times the pressure in 1988, although runs 48, 51 and 66 were close.

Criteria five, V, requires that the model predict a frost temperature of 41 K, with the non- N_2 surface at 60–65 K in 2001–2002. The frost temperature in 1993 should be in the range 38–42 K. Run 68 came closest, predicting 39 K in 1993 and in 2001–2002 40 K for the N_2 and 61 K for the frost-free surface. Run 66 also predicted temperatures reasonably close to these values. With the broad range of values in 1983 for surface temperatures all runs passed.

It might thus seem that run 48 or 68 provides the best match to observational criteria. That would imply that the properties of the surface and frost have been narrowed to a frost albedo of 0.7, a frost emissivity of 0.7, and thermal inertia between 10 and 18 J/m² s^{1/2} K. However, these two runs have narrowly peaked atmospheric pressure, and by 2013 both predict dramatic decreases in pressure, as illustrated in Fig. 3 for run 48.

To match the newest occultation results we need to look at the cases that have a broader, longer-lived peak in pressure associated with slower sublimation of the northern polar cap. With the additional results presented for the 2012 and 2013 occultations at the Pluto Conference (Olkin et al., 2013, B. Sicardy, personal communication, 2013; Person et al., this issue, 2013) run 22 came closest to matching the new observations, followed by run 12, although these runs did not have a particularly good match to the frost and surface temperatures derived for 1993 and 2001–2002.

Run 22, shown in Fig. 5, has the broadest pressure peak of the 9 best cases. The drop off in pressure predicted by this set of parameters between 2010 and 2013 is just 7%, the equivalent of flat given other uncertainties. This set of parameters predicts an atmospheric pressure of 2.4 Pa at the surface at the time of the New Horizons flyby. Run 22 had a thermal inertia = 41.8 J/m² s^{1/2} K, frost albedo = 0.8, and frost emissivity = 0.6.

Table 3

Criteria from Table 2 are listed in the last column, compared to each run. The criteria that were matched well are in bold, those which were close are italicized. Of these, runs 48 and 68 came closest to reproducing the pressure trends through 2010. The predicted pressure drops precipitously after 2010 however so they do not reproduce the most recent results. Runs 22 and 12 are the only cases that predict atmospheric pressure staying flat, not decreasing in 2012–2013, and also have a south polar cap in 1988.

Run #	Thermal Inertia (TI) (mks)	Surface albedo	Frost albedo	Frost emissivity	Atmospheric pressure in 2015 (Pa)	Criteria met
22 (best of all)	41.8	0.2	0.8	0.6	2.4	I, II, III, IV, V, VI
77	41.8	0.2	0.7	0.8	2.1	I, II, III, IV, V, VI
12	32.0	0.2	0.8	0.55	3.2	I, II, III, IV, V, VI
55	32.0	0.2	0.7	0.8	0.42	I, II, III, IV, V, VI
25	18.0	0.2	0.8	0.55	2.5	I, II, III, IV, V, VI
48	18.0	0.2	0.7	0.7	0.37	I, II, III, IV, V, VI
51	18.0	0.3	0.7	0.7	0.30	I, II, III, IV, V, VI
66	10.1	0.2	0.8	0.55	1.9	I, II, III, IV, V, VI
68	10.1	0.2	0.7	0.7	0.14	I, II, III, IV, V, VI

7.2. Discussion of limitations on model results

All observables have varying degrees of uncertainty. Atmospheric pressure has the uncertainty associated with extrapolation of pressure at the reference altitude of the occultations to the surface. Temperatures are derived from best fits to spectral data.

The shape of the occultation light curves has sometimes been attributed to the presence of haze in the atmosphere. We tested the potential effect of haze by running our best-fit case (#22) with a reduction in the solar energy term that would result from a high level haze partially blocking the Sun. The presence of a haze does modulate the pressure profile although seasonal change still dominates the overall behavior. This adds another dimension to parameter space.

Even the apparent lack of zonal bands in the images could be due to real topography on Pluto. If that is the case then significantly higher thermal inertias could be entertained, as in Young (2013), and the pressure peak could persist or even increase in 2013, although it would still be difficult to produce a south polar cap in 1988. The most substantial difference between the findings reported by Olkin et al. (2013) and those reported here is the emphasis we place on the existence of a bright south polar cap in 1988. If the bright south pole detected in 1988 is due to non-nitrogen ice then removing that constraint would also allow for higher thermal inertia cases.

Although based on the same physics the implementation of the HP96 model vs. the Young (2013) model is different, and the models do not always predict the same outcomes for the same set of input parameters. Treatment of initial conditions is different between the two. The computational “engine” is different. Resolving how the differences in implementation lead to different outcomes is left to future study.

There is also a difference in our selection criteria for “good fits”. We have chosen to emphasize the existence of a south polar cap in 1988. Olkin et al. (2013) weight the occultation results more heavily than the albedo constraints. The best judgment of our choices will come from the results from the New Horizons flyby of Pluto in 2015.

8. Predictions for New Horizons

We predict that New Horizons will see a thinning, sunlit north polar cap reaching perhaps as far south as 35N latitude. The frost-covered southern hemisphere will be bright from 10S latitude to the terminator. The frost temperature will be ~38 K, while the warmest patches on the surface will reach ~52 K.

It does not appear that the atmosphere will collapse prior to the arrival of New Horizons although pressure will be dropping as N_2 condenses on the south polar cap. The range of pressures predicted for 2015 for the nine very good cases is 0.14–3.2 Pa. The best match

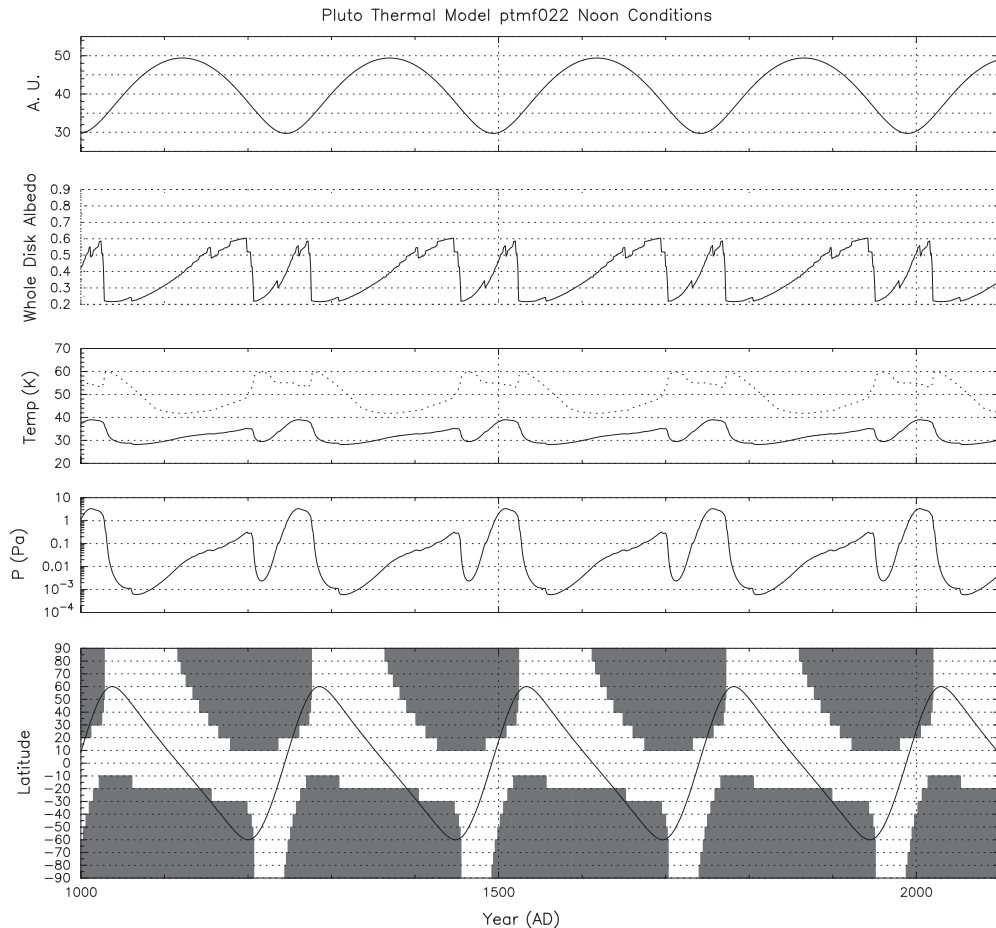


Fig. 5. Run 22 meets our criteria best when the most recent occultation results are included. It had a thermal inertia = $41.8 \text{ J/m}^2 \text{ s}^{1/2} \text{ K}$, frost albedo = 0.8, and frost emissivity = 0.6. Temperatures plotted are for the frost point and the warmest point on the surface. The atmospheric pressure is still at the peak associated with sublimation of the north polar cap, and although it is not increasing it is steady in 2013. The south polar cap has started to form in 1988. The north polar cap has a greater latitudinal extent than the south polar cap in 1994. It persists through 2015, delaying the expected plummet in atmospheric pressure to after the New Horizons flyby.

predicts that New Horizons will detect an atmospheric pressure of 2.4 Pa.

Acknowledgment

This task was supported by a NASA Outer Planet Research Program grant.

References

- Binzel, R.P., Mulholland, J.D., 1983. Photometry of Pluto during the 1982 opposition. *Astron. J.* 88, 222–225.
- Bosh, A. et al., 2013. The State of Pluto's Atmosphere in 2012–2013. *Bull. Am. Astron. Soc.* 45, 404.
- Buie, M.W., Tholen, D.J., Horne, K., 1992. Albedo maps of Pluto and Charon: Initial mutual event results. *Icarus* 97, 211–227.
- Buie, M.W., Grundy, W.M., Young, E.F., Young, L.A., Stern, S.A., 2010a. Pluto and Charon with the Hubble Space Telescope. I. Monitoring global change and improved surface properties from light curves. *Astron. J.* 139, 1117–1127.
- Buie, M.W., Grundy, W.M., Young, E.F., Young, L.A., Stern, S.A., 2010b. Pluto and Charon with the Hubble Space Telescope. II. Resolving changes on Pluto's surface and a map for Charon. *Astron. J.* 139, 1128–1143.
- Cruikshank, D. et al., 1976. Pluto: Evidence for methane frost. *Science* 194, 835–837.
- Douté, S., Schmitt, B., Quirico, E., Owen, T.C., Cruikshank, D.P., de Bergh, C., Geballe, T.R., Roush, T.L., 1999. Evidence for methane segregation at the surface of Pluto. *Icarus* 142, 421–444.
- Elliot, J., Young, L.A., 1991. Occultation Constraints on Atmospheric Models for Pluto. *Bull. Am. Astron. Soc.* 23, 1216.
- Elliot, J.L., Young, L.A., 1992. Analysis of stellar occultation data for planetary atmospheres: I. Model fitting with application to Pluto. *Astron. J.* 103, 991–1015.
- Elliot, J. et al., 1989. Pluto's radius and atmosphere: Results from the entire 9 June 1988 occultation data set. *Icarus* 77, 148–170.
- Elliot, J.L. et al., 2003. The recent expansion of Pluto's atmosphere. *Nature* 424, 165–168.
- Elliot, J.L. et al., 2007. Changes in Pluto's atmosphere: 1988–2006. *Astron. J.* 134, 1–13.
- Eshleman, V.R., 1989. Pluto's atmosphere: Models based on refraction, inversion, and vapor–pressure equilibrium. *Icarus* 80, 439–443.
- Grundy, W.M., Buie, M.W., 2001. Distribution and evolution of CH_4 , N_2 , and CO ices on Pluto's surface: 1995 to 1998. *Icarus* 153, 248–263.
- Grundy, W.M., Olkin, C.B., Young, L.A., Holler, B.J., 2014. Near-infrared spectral monitoring of Pluto's ices II: Recent decline of CO and N_2 ice absorptions. *Icarus* (arXiv:1402.4842).
- Hansen, C.J., Paige, D.A., 1992. A thermal model for the seasonal nitrogen cycle on Triton. *Icarus* 99, 273–288.
- Hansen, C.J., Paige, D.A., 1996. Seasonal nitrogen cycles on Pluto. *Icarus* 120, 247–265.
- Hubbard, W., Yelle, R., Lunine, J., 1990. Non-isothermal Pluto atmosphere models. *Icarus* 84, 1–11.
- Leighton, R., Murray, B., 1966. Behavior of carbon dioxide and other volatiles on Mars. *Science* 153, 136–144.
- Lellouch, E. et al., 2009. Pluto's lower atmosphere structure and methane abundance from high-resolution spectroscopy and stellar occultations. *Astron. Astrophys.* 495, L17–L21.
- Lellouch, E., Stansberry, J., Emery, J., Grundy, W., Cruikshank, D.P., 2011a. Thermal properties of Pluto's and Charon's surfaces from Spitzer observations. *Icarus* 214, 701–716.
- Lellouch, E., de Bergh, C., Scardy, B., Kaeufl, H.U., Smette, A., 2011b. High resolution spectroscopy of Pluto's atmosphere: Detection of the $2.3 \mu\text{m}$ CH_4 bands and evidence for carbon monoxide. *Astron. Astrophys.* 530, 1–5.
- Marcialis, R.L., 1988. A two-spot albedo model for the surface of Pluto. *Astron. J.* 95, 941–947.
- Olkin, C.B. et al., 2007. Pluto's spectrum from 1.0 to $4.2 \mu\text{m}$: Implications for surface properties. *Astron. J.* 133, 420–431.
- Olkin, C.B. et al., 2013. Pluto's atmosphere does not collapse. arXiv: 1309.08410.

- Owen, T. et al., 1992. Detection of nitrogen and carbon monoxide on the surface of Pluto. *Bull. Am. Astron. Soc.* 24, 961.
- Owen, T. et al., 1993. Surface ices and the atmospheric composition of Pluto. *Science* 261, 745–748.
- Pasachoff, J.M. et al., 2005. The structure of Pluto's atmosphere from the 2002 August 21 stellar occultation. *Astron. J.* 129, 1718–1723.
- Person, M.J. et al., 2013. The 2011 June 23 stellar occultation by Pluto: Airborne and ground observations. *Astron. J.* 146, 83. <http://dx.doi.org/10.1088/0004-6256/146/4/83>.
- Schaefer, B.E., Buie, M.W., Smith, L.T., 2008. Pluto's light curve in 1933–1934. *Icarus* 197, 590–598.
- Sicardy, B. et al., 2003. Large changes in Pluto's atmosphere as revealed by recent stellar occultations. *Nature* 424, 168–170.
- Spencer, J., 1990. Nitrogen frost migration on Triton: A historical model. *Geophys. Res. Lett.* 17, 1769–1772.
- Spencer, J.R., Moore, J.M., 1992. The influence of thermal inertia on temperatures and frost stability on Triton. *Icarus* 99, 261–272.
- Stansberry, J.A., Lunine, J.I., Hubbard, W.B., Yelle, R.V., Hunten, D.M., 1994. Mirages and the nature of Pluto's atmosphere. *Icarus* 111, 503–513.
- Stern, A., Trafton, L., 1984. Constraints on bulk composition, seasonal variation and global dynamics of Pluto's atmosphere. *Icarus* 57, 231–240.
- Stern, S.A., Buie, M.W., Trafton, L.M., 1997. HST high-resolution images and maps of Pluto. *Astron. J.* 113, 827–843.
- Sykes, M., 1993. Implications for Pluto–Charon radiometry. *Bull. Am. Astron. Soc.* 25, 1138.
- Sykes, M., Cutri, R., Lebofsky, L., Binzel, R., 1987. IRAS serendipitous survey observations of Pluto and Charon. *Science* 237, 1336–1340.
- Trafton, L., 1984. Large seasonal variations in Triton's atmosphere. *Icarus* 58, 312–324.
- Tryka, K.A., Brown, R.H., Cruikshank, D.P., Owen, T.C., Geballe, T.R., deBergh, C., 1994. Temperature of nitrogen ice on Pluto and its implication for flux measurements. *Icarus* 112, 513–527.
- Ward, W.R., 1974. Climatic variations on Mars: 1. Astronomical theory of insolation. *J. Geophys. Res.* 79, 3375–3386.
- Young, L.A., 2013. Pluto's seasons: New predictions for New Horizons. *Astrophys. J.* 766, L22. <http://dx.doi.org/10.1088/2041-8205/766/2/L22>.
- Young, E.F., Binzel, R.P., 1993. Comparative mapping of Pluto's sub-Charon hemisphere: Three least squares models based on mutual event lightcurves. *Icarus* 102, 134–149.
- Young, E.F. et al., 2008. Vertical structure in Pluto's atmosphere from the 2006 June 12 stellar occultation. *Astron. J.* 136, 1757–1769.
- Young, L. et al., 2010. Results from the 2010 February 14 and July 4 Pluto occultations. *Bull. Am. Astron. Soc.* 42, 982.